Electric Power Systems Research 117 (2014) 104–114

Contents lists available at ScienceDirect

Electric Power Systems Research

journal homepage: www.elsevier.com/locate/epsr

Application of DSTATCOM for surplus power circulation in MV and LV distribution networks with single-phase distributed energy resources

Farhad Shahnia*, Ruwan P.S. Chandrasena, Arindam Ghosh, Sumedha Rajakaruna

Department of Electrical and Computer Engineering, Curtin University, Perth, Australia

ARTICLE INFO

Article history:
Received 11 February 2014
Received in revised form 27 June 2014
Accepted 12 August 2014
Available online 29 August 2014

Keywords:
Distribution static compensator (DSTATCOM)
Distributed energy resource (DER)
Power circulation
Single-phase DERs
Low voltage feeders
Medium voltage feeders

ABSTRACT

Single-phase distributed energy resources (DERs), such as rooftop photovoltaic arrays, are usually installed based on the need and affordability of clients without any regard to the power demand of the connected phase of a three-phase system. It might so happen that the power generation in a particular phase is more than its load demand. This may cause a reverse power flow in a particular phase, especially in a three-phase, four-wire distribution system. If now the load demand in the other two phases is more than their respective generations, then these two phases will see a forward power flow, while there will be a reverse power flow in the third phase. This will create severe unbalance in the upstream network. In this paper, a distribution static compensator (DSTATCOM) is used to circulate the excess generation from one phase to the others such that a set of balanced currents flow from or into the upstream network. Two different topologies of DSTATCOM are proposed in this paper for the low and medium voltage feeders. Two different power circulation strategies are developed for this purpose. Furthermore, a suitable feedback scheme is developed for each topology for power converter control. The performance of the proposed topologies and the control schemes for the DSTATCOM is evaluated through computer simulation studies using PSCAD/EMTDC.

1. Introduction

Distributed generation on both low voltage (LV) and medium voltage (MV) feeders has increased rapidly over the last decade mainly due to the recent global efforts to minimize carbon emissions and to increase power system efficiency and reliability [1–6]. Solar photovoltaic (PV) is the most popular form of renewable distributed generation (DG), especially in countries with abundance of sunlight and government subsidies for renewable energy generation [7–13]. Other forms of DGs, such as micro wind turbines, fuel cells, microturbines and bio-diesel engines, are also been deployed in various parts of the world. Furthermore, electric vehicles (EVs) are expected to make a significant percentage of the load in the near future [14,15]. At the present time, the EVs only charge their batteries by drawing power from the grid in grid-to-vehicle (G2V) mode [16]. However, as the battery technology improves, EVs can work as DGs, where they supply power from the batteries to the grid in vehicle-to-grid (V2G) mode [17,18]. Moreover, energy storage devices such as battery banks and flywheels are expected to penetrate into the grid to regulate the energy fluctuations arising from intermittent renewable sources [19–22]. All these different generating sources and energy storages that can feed power to the grid are collectively referred to as distributed energy resource (DER).

Despite the well-known advantages of DERs such as reduced transmission losses, increased reliability etc., their introduction in LV feeders has some drawbacks in terms of power quality that need to be addressed [23–25]. Some of these are voltage/current unbalance among phases and voltage rise [26]. Although the utility grid supplies balanced voltages to the LV feeders, unequal distribution of single-phase DERs may create some current unbalance in LV feeders [27]. For example, in Australia, single-phase solar PVs are increasingly getting connected to LV feeders in a random fashion. Their ratings can also vary. This can ultimately affect the upstream MV feeder since large unbalanced currents can be drawn from it.

One method of eliminating the voltage unbalance and improving the voltage profile in the distribution feeders is applying a new control technique for the DERs' converters such that not only power transfer is facilitated but also power quality is enhanced in the network. As an example, in [27], a new converter control topology is proposed for the single-phase PV converters. Alternatively, a droop control technique is proposed for improving the voltage profile in LV feeders by the help of PV converters in [28]. Similarly, for three-phase DERs, a converter control strategy is proposed in [29] such that not only it facilitates the power flow from the DER

* Corresponding author. Tel.: +61 432 020 732.
E-mail address: farhad.shahnia@curtin.edu.au (F. Shahnia).

http://dx.doi.org/10.1016/j.epsr.2014.08.010
0378-7796/

to the network but it also compensates the voltage at its terminals although the network loads are unbalanced.

On the other hand, custom power devices (CPDs) have already been proven to be effective for alleviating power quality problems [30]. Different configurations, topologies and control algorithms are already proposed for them. As an example, in [31], it is shown that distribution static compensators (DSTATCOM) and dynamic voltage regulators (DVR) are effective types of CPDs for power quality enhancement in LV feeders. The DSTATCOM and DVR in [31] are composed of three single-phase converters connected to the same DC bus. In [32], it is shown that unified power quality conditioner (UPQC), an another type of CPDs, which is composed of two back-to-back connected series and parallel converters, can enhance the power quality in MV feeders. In [33,34], a UPQC configuration is utilized for the interfacing converter of a DER to enable active power flow as well as voltage unbalance improvement in the network. In [35] it is shown that an open UPQC, where the series and parallel converters are located with some distance and are not connected back-to-back, can be used in MV/LV substations to enhance the power quality. In [36,37], it is shown that an interline DVR and interline UPQC can facilitate power flow from one MV feeder to another MV feeder as well as enhancing power quality in the feeders.

Among the above discussed CPDs, DSTATCOM is highly successful in different power quality issues such as improving power factor by reactive power injection, controlling the voltage at the interconnected bus and suppressing harmonic currents [38–40]. Some of these issues such as harmonics and power losses have already been investigated in the context of DERs. It has been shown in [41] that a DSTATCOM can reduce voltage unbalance in a distribution feeder. Furthermore, the best possible location for installing a DSTATCOM for optimum performance was also investigated in [31].

Since the single-phase DERs are placed randomly among the phases, it is possible that the generation in a particular phase exceeds the load demand in that phase. Under such a condition, the surplus phase power will feed back towards the distribution transformer in the LV feeders. Rooftop PVs are a good example of the single-phase DERs that generate the maximum amount of power at midday when the residential load demand is at its minimum. Hence, the LV feeders in such cases can experience a reverse power flow in one or more phases. It is to be noted that this reverse power flow is a steady-state phenomenon and is not a transient issue. Assuming a residential area with a high penetration level of PVs, it can be expected that the reverse power flow will not only be observed in the LV feeders but it will also be observed in the MV feeder supplying these LV feeders. In [41,42], application of a DSTATCOM, connected to the MV feeder, is been considered for circulating surplus phase power from one phase to another. This is a new application for DSTATCOM.

A DSTATCOM can be connected to LV as well as MV feeders. The main advantage of installing a DSTATCOM in an LV feeder is the elimination of the reverse power flow at the point of emergence of the problem. This is the most effective way to prevent the reverse power flow before it being injected to the MV side. However, installation of a few DSTATCOMs in several adjoining LV feeders, supplied by the same MV line, is not cost-effective. Hence, reduction in the initial investment costs is the main advantage of installing a DSTATCOM in the MV feeder. In general, several criteria can be considered in choosing the connection of DSTATCOM to a LV or MV feeder such as:

- *Economic concerns*: The cost of a DSTATCOM is highly dependent on its rating. Similar to other electrical devices, this cost increases significantly by the increase in the DSTATCOM rating. Hence, economic analyses can lead to choosing among the two options of installing one DSTATCOM, with a higher rating, in the MV feeder or several DSTATCOMs, each with a smaller rating, in the LV feeders.
- *The level and frequency of reverse power flow in the feeder*: The reverse power flow may be experienced more frequently with higher percentage in the LV feeders while it may neither be very frequent nor a high percentage in the MV feeders. Therefore, the level of reverse power flow in MV line can sometimes be insignificant while it is significant in some LV lines.
- *Reliability concerns*: Failure of a DSTATCOM in a LV feeder may only interrupt the power supply to a few customers in the feeder, however; its failure in a MV feeder may result in power interruption to a larger number of customers of the MV feeder.
- *Operational and maintenance (O&M) concerns*: A DSTATCOM installed in a LV feeder will have less O&M costs and lower hazards for the personnel under hot line practices, in comparison to those of the MV installation.

The DC link of the DSTATCOM, used in [31,40–42], consists of a battery (i.e. a DC source). Therefore, the DSTATCOM can operate like an uninterruptable power supply (UPS) where it can exchange active as well as reactive power with the feeder. In this paper, to minimize the initial and O&M costs of a DSTATCOM, a DC capacitor is used instead of the battery. The main difference in this case is that the DSTATCOM only exchanges reactive power with the feeder to facilitate current circulation from one phase to another. However, the voltage across the capacitor should be controlled to a rated value by drawing active power from the AC network. Unless the voltage across the DC capacitor regulated at its rated value, the DSTATCOM is not able to produce the desired output and will fail to circulate the reverse flowing power/current.

Two different topologies are considered for the DSTATCOM in this paper – one when used in LV feeder and the other is used in MV feeder. The positioning of the boosting transformer in the output of the DSTATCOM is different for MV and LV applications. This changes the filter characteristic in the output of the DSTATCOM. In this paper, it has been shown that voltage control strategy is suitable for LV applications from the output passive filter arrangement point of view. On the other hand, it is shown that current control strategy is well suited for MV applications, from the same point of view.

The current and voltage output references of the DSTATCOM are generated such that a set of balanced currents are drawn from the upstream side, while facilitating the circulation of reverse flowing power among the phases. In addition, the used topology for LV application provides a reliable path between the phases for off-grid applications. Hence, the single-phase DERs, controlled in droop, can manage the power demand of the three-phase network when the LV feeder is isolated from the upstream side, irrespective of the phase to which they are connected. This application is not considered in [31,40–42].

The main aim of the DSTATCOM, either in LV or in MV, is to force the upstream currents balanced irrespective of the power flow in its downstream side. To achieve this, the DSTATCOM must circulate power from one phase to the other. In other words, it forces the power from the phase with excess generation to flow in the other phase(s) to avoid reverse power flow in that phase. Even when there is no reverse power flow and the power to the load is supplied by the grid, the DSTATCOM balances the upstream currents, but this also occurs as the power is circulated amongst the phases.

The main novelty of this paper is in the application of DSTATCOM to circulate power/current among the phases in a network where unbalanced reverse power flow is observed in one or more phases. This is considered as the main objective of DSTATCOM

functionality in this paper. Proper DSTATCOM filter arrangements are considered, separately when it is connected to an LV or an MV feeder. Based on the filter arrangements, suitable control techniques are developed. From the output passive filter arrangement point of view, in this paper, it is shown that voltage control strategy is more suitable for the DSTATCOM when it is connected to the LV feeder, while the current control strategy is better suited when it is connected to the MV feeder. The main contribution of this paper is providing the guidelines for selecting DSTATCOM filter arrangement and its converter control strategies, for the LV and MV applications to enhance power circulation among the phases. The performance of the proposed topologies and the control schemes for the DSTATCOM, to circulate power from one phase to another in the LV/MV feeders with unbalanced reverse power flow, is evaluated through numerical analyses based on PSCAD/EMTDC.

2. DSTATCOM topologies

For the application mentioned in this paper, the DSTATCOM should be able to circulate power between the phases through a common DC bus. The chosen DSTATCOM structures are composed of a voltage source converter (VSC), as shown in Fig. 1. The DSTATCOM contains three single-phase full bridges, referred to as H-bridge VSCs, supplied from a common DC bus. The output of each H-bridge is connected to an LC filter, consisting of an inductor (L_f) and a capacitor (C_f). To provide galvanic isolation, three single-phase transformers, with a turns ration of 1:a, are connected between the output of each H-bridge and the LC filter. These transformers, connected in star in their secondary sides, also provide voltage boosting. In Fig. 1(a), the resistance R_f represents the switching and transformer losses. The filter capacitor C_f is directly connected to the feeder. This is a suitable topology for the DSTATCOM when installed in LV side.

When installing the DSTATCOM in MV feeders, the VSC and filter are desired to be operated in low voltage and connected to the MV feeder through a transformer with appropriate turns ratio. Hence, the transformers are connected between the filter capacitor and the MV feeder, as shown in Fig. 1(b).

The proposed DSTATCOM, when connected to the LV feeder, has a three-phase four-wire configuration; however, when connected to the MV feeder, has a three-phase three-wire configuration. It is to be noted that the VSC structure is not the main focus of this research. Although three single-phase VSCs are considered in this paper, any 3-leg or 4-leg VSCs which can provide zero sequence circulation can also be used. The main advantage of the utilized three single-phase VSCs is that each phase of the DSTATCOM output can be controlled individually and independently without affecting the other phases. However, it has slightly higher costs compared to 3-leg and 4-leg configurations due to the higher number of power electronic switches.

In order to provide galvanic isolation between the DC bus and the AC system, a transformer can be utilized at the output of the VSCs. This is valid for any VSC configuration. The transformer can also provide voltage boosting. It is to be noted that voltage boosting is not required when the DSTATCOM is connected to the LV feeder and its DC bus voltage is more than the AC side peak voltage. However, if the DC bus voltage is less than the AC side peak voltage or when the DSTATCOM is connected to the MV feeder, voltage boosting transformers are required.

Two different control algorithms are proposed for controlling the DSTATCOM – the first when it is used in LV feeders and the second when it is installed in MV feeders, which are discussed in detail in Section 3.

3. Power circulation strategies

Two different power circulating strategies are proposed and considered, one for each topology.

3.1. Power circulation strategy for DSTATCOM in LV feeders

It is desired that the DSTATCOM is operated in a fashion such that a set of balanced currents is observed in the upstream side. It is assumed that the loads are connected to a LV (typically 415 V) feeder, supplied through an MV (typically 11 kV) feeder from a substation. The substation will be considered as source and its voltage is assumed to be balanced. The DSTATCOM is connected to the LV feeder. To have a balanced set of current flowing in the MV feeder, the voltage at the point of common coupling (PCC) of the DSTATCOM must be balanced. This can be achieved by controlling the DSTATCOM such that it generates and holds a balanced set of voltage at its PCC. A voltage control technique is utilized to hold a balanced set of voltages across the three filter capacitors (C_f). The three-phase reference voltage will then be [32]

$$[\boldsymbol{V}_{cf}]^{ref}_{ABC} = E_{DSTAT} \angle \delta^{ref}_{cf,A} \times [\,1 \quad \lambda^2 \quad \lambda\,]^T \tag{1}$$

where E_{DSTAT} is the desired phase RMS voltage for the PCC (i.e. 240 V in this study), $\delta_{cf,A}$ is the angle of the terminal voltage, v_{TA} and $\lambda = 1 \angle 120^\circ$. This voltage is used as the reference for converter control, as discussed in the next section. The DSTATCOM exchanges reactive power with the LV feeder to hold the desired voltage at its PCC.

The main assumption above is the presence of a balanced voltage at the secondary side of the distribution transformer. This may not be true in a real network where a MV feeder supplies several LV feeders and each LV feeder injects some reverse power into the MV feeder. In such a case, the MV feeder may induce unbalanced voltages to the secondary side of the distribution transformer. Hence, installing one DSTATCOM at one of the LV feeders will not guarantee a set of balanced currents to flow in the upstream of the DSTATCOM. Thereby, a DSTATCOM is required to be installed in every LV feeder in which single-phase DERs are connected. This will restrict the injection of reverse power flow into the MV feeder.

The operation of the DSTATCOM depends on the voltage variations across the DC capacitor (V_{dc}). Any load change in the feeder is a disturbance to the DSTATCOM controller and results in a voltage fluctuation in V_{dc}. This voltage fluctuation corresponds to the change in the active power flow between the DC capacitor and the feeder. V_{dc} can be kept constant and equal to its reference value if the DC capacitor does not exchange any power with the feeder [30]. For this, the angle of the voltage across the AC filter capacitor (δ_{cf}) must be varied with respect to the variations in V_{dc} as per

$$\delta^{ref}_{cf} = \left(k_P + \frac{k_I}{s}\right)(V^{ref}_{dc} - V_{dc}) \tag{2}$$

Therefore, for any fluctuation in V_{dc} following a load change in the feeder, δ_{cf} is modified such that V_{dc} is regulated to its reference (V^{ref}_{dc}). Note that in such a case, the DSTATCOM will only absorb a small amount of active power from the feeder which is equal to the losses in its H-bridges and transformers.

It is to be noted that, in general, the LV feeders are more resistive than inductive. For example, in Australia, the typical LV feeders have an $R/X \approx 2$–3 [43]. Under such scenarios, it is possible that the DSTATCOM cannot effectively control its PCC voltage to the desired value by only exchanging reactive power with the feeder. This problem can be addressed if the DSTATCOM utilizes a DC source (e.g. a battery) instead of a DC capacitor in such scenarios, to facilitate active power exchange with the feeder.

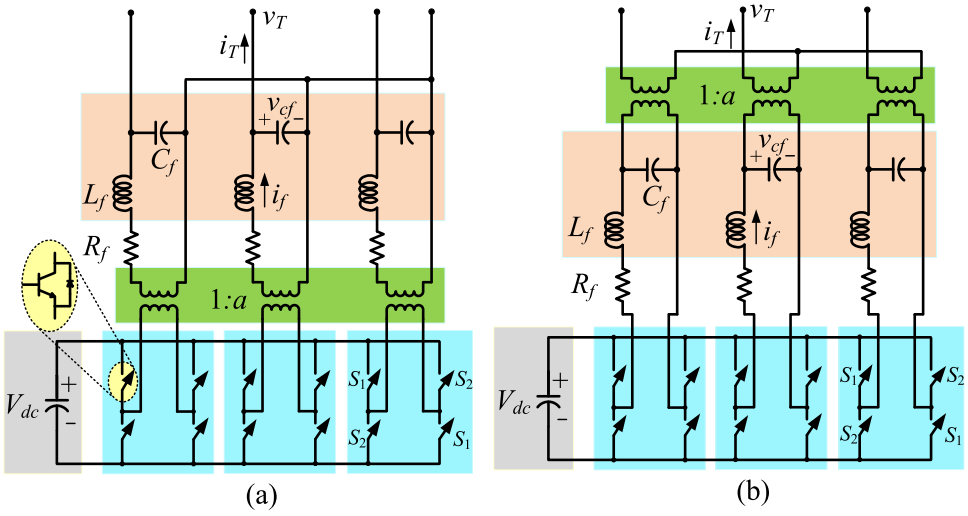

Fig. 1. DSTATCOM toplogy with power circulation capability to be installed in: (a) LV feeders, (b) MV feeders.

3.2. Power circulation strategy for DSTATCOM in MV feeders

Now, let us assume that the DSATATCOM is connected to the MV feeder. A voltage control strategy, similar to the abovementioned case, can be utilized. However, in Section 5, through simulation studies, it will be shown that although the DSTATCOM will have an acceptable level of tracking of the voltage across C_f, due to the leakage inductance of the coupling transformers, the DSTATCOM PCC voltage is not perfectly balanced. Hence, a balanced set of currents will not be observed in the upstream side.

To avoid this problem, a current control strategy is utilized. In this method, the proper references for the output current for each phase of the DSTATCOM are calculated and the DSTATCOM is controlled to ensure the desired current is injected into the PCC.

The reference output currents of the DSTATCOM are generated such that power circulation between the phases. As a consequence, the upstream currents become balanced. For this purpose, the theory of instantaneous symmetrical component is utilized [44]. To apply the theory, first the fundamental positive sequence of the PCC voltage is obtained [45]. Let the instantaneous positive sequence voltages be denoted by v_{A1}, v_{B1} and v_{C1}. The reference currents can then be calculated as [46]

$$[\boldsymbol{i}_T]^{ref}_{ABC} = [\boldsymbol{i}_L]_{ABC} - \frac{v_{A1}i_{LA} + v_{B1}i_{LB} + v_{C1}i_{LC}}{v^2_{A1} + v^2_{B1} + v^2_{C1}}[\boldsymbol{v}_1]_{ABC} \tag{3}$$

where i_L is the current in the downstream of DSTATCOM. This current is used as the reference for converter control, discussed in the next section.

4. Converter switching control

As discussed in Section 3, based on the filter topologies in the output of VSCs, a voltage control technique is preferred when DSTATCOM is connected to LV feeders and a current control technique is preferred when it is connected to MV feeders. Proper reference tracking technique for each mode is described in details below.

4.1. Voltage control technique

Let us consider only one phase of the DSTATCOM circuit in Fig. 1(a), in which the state vector is defined as [47]

$$\boldsymbol{x}(t) = [\, v_{cf}(t) \quad i_f(t) \,]^T \tag{4}$$

where $v_{cf}(t)$ represent the instantaneous voltage across AC filter capacitor, $i_f(t)$ is the current passing through filter inductor L_f and T is the transpose operator. Then, the equivalent circuit of this system can be represented with state space description of

$$\dot{\boldsymbol{x}}(t) = \boldsymbol{A}x(t) + \boldsymbol{B}_1 u_c(t) + \boldsymbol{B}_2 i_T(t) \tag{5}$$

where

$$\boldsymbol{A} = \begin{bmatrix} 0 & \frac{1}{C_f} \\ -\frac{1}{L_f} & -\frac{R_f}{L_f} \end{bmatrix} \quad \boldsymbol{B}_1 = \begin{bmatrix} 0 & \frac{a.Vdc}{L_f} \end{bmatrix}^T \quad \boldsymbol{B}_2 = \begin{bmatrix} -\frac{1}{C_f} & 0 \end{bmatrix}^T$$

are system matrices, $u_c(t)$ is the continuous-time version of switching function u and $i_T(t)$ represents the effect of the network transients on the converter. Hence, it is assumed to be an exogenous disturbance input to the system and will be neglected when designing the controller.

In the control system, the desired values for each control parameter in the steady state condition must be known. However, it is rather difficult to determine the reference for i_f in (4). Nevertheless, it is desired that i_f has only low frequencies and its high frequency components ($\tilde{i}_f$) are zero. Therefore, instead of using i_f as a control parameter, $\tilde{i}_f$ is used in the control system. In [47], it is shown that $\tilde{i}_f$ can be obtained utilizing a high pass filter, where its desired reference is chosen equal to zero.

Eq. (2) can be represented in discrete-time domain as [48]

$$\begin{aligned} \boldsymbol{x}(k+1) &= \boldsymbol{F}\boldsymbol{x}(k) + \boldsymbol{G}_1 u_c(k) + \boldsymbol{G}_2 i_T(k) \\ y(k) &= \boldsymbol{C}\boldsymbol{x}(k) \end{aligned} \tag{6}$$

where

$$\boldsymbol{F} = e^{A.T_s}, \quad \boldsymbol{G}_1 = \int_0^{T_s} e^{At}\boldsymbol{B}_1 dt, \quad \boldsymbol{G}_2 = \int_0^{T_s} e^{At}\boldsymbol{B}_2 dt$$

and T_s is the sampling time. Using a suitable state feedback control law, $u_c(k)$ can be computed as

$$u_c(k) = -\boldsymbol{K}[\boldsymbol{x}(k) - \boldsymbol{x}_{ref}(k)] \tag{7}$$

where $\boldsymbol{K} = [k_1\ k_2]$ is the gain matrix and $x_{ref}(k)$ is the desired state vector in discrete-time mode, expressed as

$$\boldsymbol{x}_{ref} = [\, v^{ref}_{cf} \quad \tilde{i}_{f,ref} \,]^T = [\, v^{ref}_{cf} \quad 0 \,]^T \tag{8}$$

It is to be noted that the desired reference value for $v_{cf}(t)$ is determined by (1).

(a) LV feeders, (b) MV feeders.

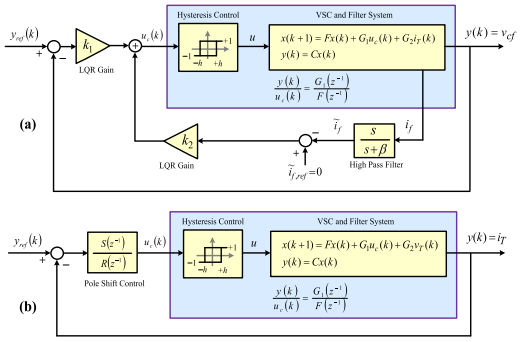

Fig. 2. Closed-loop switching control block diagram for: (a) voltage control strategy based on LQR, (b) current control strategy based on pole-shift.

As the system behaviour in the steady-state is of importance and assuming a full control over $u_c(k)$, an infinite time linear quadratic regulator (LQR) [49] is designed for this problem to define $\boldsymbol{K}$. This controller is more stable than PID controllers. In addition, PID controllers are not very effective when they are utilized in time-varying references.

In a discrete LQR problem, an objective function J is chosen as [49]

$$J(k) = \sum_{k=0}^{\infty} [(\boldsymbol{x}(k) - \boldsymbol{x}_{ref}(k))^T \boldsymbol{Q}(k)(\boldsymbol{x}(k) - \boldsymbol{x}_{ref}(k)) + u_c(k)^T R(k) u_c(k)] \tag{9}$$

where R is the control cost, Q is the state weighting matrix which reflects the importance of each controlling parameter in $\boldsymbol{x}$ and $J(\infty)$ represents the objective function at infinite time (steady-state condition) for the system. Eq. (9) is then minimized to obtain the optimal control law $u_c(k)$ through solution of steady state Riccati equations [49]. The LQR method ensures the desired system performance provided that the variations of system load and source parameters are within acceptable limits.

Eq. (7) gives the total tracking error of the converter. The tracking error can be minimized by limiting this error within a very small bandwidth (e.g. $h = 10^{-4}$). Now, from (7), the switching function u (i.e. which pairs of IGBTs to turn ON/OFF) is generated using a hysteresis error control as

$$\begin{aligned} &\text{If} \quad u_c(k) > +h \quad &&\text{then} \quad u = +1 \\ &\text{If} \quad -h \le u_c(k) \le +h \quad &&\text{then} \quad u = \text{previous } u \\ &\text{If} \quad u_c(k) < -h \quad &&\text{then} \quad u = -1 \end{aligned} \tag{10}$$

If $u = 1$, then S_1 pair of IGBTs turn ON and if $u = -1$, then S_2 pair of IGBTs turn ON. This switching control is considering only one phase. Similar switching action is also employed for the other two phases, separately.

Note that the switching frequency of IGBTs depends on the value of h. On the other hand, the power loss in the IGBTs depends on their switching frequency and therefore on h. Although reducing h to smaller values improves the reference tracking by the converter, it might lead to very high impractical switching frequencies and high switching losses. Therefore, h is to be defined such that a proper reference tracking is achieved while the switching frequency and power losses in the VSC are acceptable [30].

The closed-loop block diagram of the control system is shown in Fig. 2(a).

4.2. Current control technique

Let us consider only one phase of the DSTATCOM circuit in Fig. 1(b), in which the state vector is defined as [40]

$$\boldsymbol{x}(t) = \begin{bmatrix} i_T(t) & i_f(t) & v_{cf}(t) \end{bmatrix}^T \tag{11}$$

where i_T is the output current of the DSTATCOM. Then, the state space equation of the system is written as

$$\begin{aligned} \dot{\boldsymbol{x}}(t) &= \boldsymbol{A}\boldsymbol{x}(t) + \boldsymbol{B}_1 u_c(t) + \boldsymbol{B}_2 v_T(t) \\ y(t) &= \boldsymbol{C}\boldsymbol{x}(t) \end{aligned} \tag{12}$$

where

$$\boldsymbol{A} = \begin{bmatrix} 0 & 0 & \frac{a}{L_T} \\ 0 & -\frac{R_f}{L_f} & -\frac{1}{aL_f} \\ -\frac{a}{C_f} & \frac{a}{C_f} & 0 \end{bmatrix}, \quad \boldsymbol{B}_1 = \begin{bmatrix} 0 & \frac{V_{dc}}{aL_f} & 0 \end{bmatrix}^T,$$

$$\boldsymbol{B}_2 = \begin{bmatrix} -\frac{1}{L_T} & 0 & 0 \end{bmatrix}^T, \quad \boldsymbol{C} = \begin{bmatrix} 1 & 0 & 0 \end{bmatrix}$$

are system matrices and $v_T(t)$ is an exogenous disturbance input to the system that is neglected when designing the controller.

As the system behaviour is governed by the poles of its transfer function (i.e. the eigenvalues of matrix $\boldsymbol{A}$), it is often desirable to modify the poles of the system in order to obtain certain properties such as rise/settling time, damping, overshoot and stability. In this paper, the control system is designed using a discrete-time output feedback pole-shift control [31]. In this technique, the open-loop poles are shifted radially towards the origin (i.e. more stable locations) to form the closed-loop poles. Similar to (6), Eq. (12) is represented in discrete-time domain. Assuming the feedback control has the form of Fig. 2(b), the system of converter and filter is represented in transfer function domain as

$$\frac{y(k)}{u_c(k)} = \frac{G_1(z^{-1})}{F(z^{-1})} = \frac{g_1 z^{-1} + g_2 z^{-2} + g_3 z^{-3} + \ldots}{1 + f_1 z^{-1} + f_2 z^{-2} + f_3 z^{-3} + \ldots} \tag{13}$$

where z^{-1} is the delay operator. Now, let the control law be given by

$$u_c(k) = \frac{S(z^{-1})}{R(z^{-1})}\{y_{ref}(k) - y(k)\} \tag{14}$$

where y_{ref} is the desired (reference) output current. From Fig. 2(b), the closed-loop characteristic equation of the system, $\Delta(z^{-1})$, is given as

$$\Delta(z^{-1}) = F(z^{-1})R(z^{-1}) + G(z^{-1})S(z^{-1}) \tag{15}$$

Unlike the pole-placement technique where $\Delta(z^{-1})$ is predefined by the user, pole-shift technique takes the form of

$$\Delta(z^{-1}) = F(\lambda z^{-1}) = 1 + \lambda f_1 z^{-1} + \lambda^2 f_2 z^{-2} + \lambda^3 f_3 z^{-3} + \ldots \tag{16}$$

where the poles are shifted by λ towards origin. In this technique, the closed-loop poles are obtained by multiplying the open-loop eigenvalues by $0 < \lambda < 1$ where λ is a scalar, close to one (e.g. $\lambda = 0.8$), which is called the pole-shift factor. The pole-shift factor is the only parameter to be defined in the controller and its value determines the control gain. It is adjusted such that the controller is limited only for the first few swings following a large impact on the system. Given β is the absolute of the largest characteristic root of $F(z^{-1})$, for guaranteeing the closed-loop system stability, λ is limited as [50]

$$-\frac{1}{\beta} < \lambda < \frac{1}{\beta} \tag{17}$$

Since the penalty on control action can be easily adjusted by λ as in (17), the closed-loop system will unlikely be instable. This is an advantage of the pole-shift technique compared to other techniques such as deadbeat control which forces all the closed-loop poles to the origin, requiring excessive control effort.

Equating (16) with (15), the controller coefficients in $R(z^{-1})$ and $S(z^{-1})$ can be obtained. For the system of converter and filter under consideration in this paper, based on the system order in (12)-(13), $S(z^{-1})$ and $R(z^{-1})$ in (14) are of the form

$$\frac{u_c(k)}{y_{ref}(k)-y(k)} = \frac{S(z^{-1})}{R(z^{-1})} = \frac{s_0+s_1z^{-1}+s_2z^{-2}}{1+r_1z^{-1}+r_2z^{-2}} \tag{18}$$

Based on these calculated values, the reference tracking error, $u_c(k)$ is defined from (18) and used to achieve a reference tracking error less than the maximum specified as described in (10). The closed-loop control configuration is shown in Fig. 2 (b).

4.3. Summary of converter switching control

A voltage control strategy, based on [31], is developed and utilized for the DSTATCOM when connected in LV feeders, as discussed in Section 3.1. Also, a current control strategy is developed and utilized, based on [46], when the DSTATCOM is connected to the MV feeder, as discussed in Section 3.2. The reference for voltage output and current output in each case is as given in (1) and (3), respectively. The switching control of the VSCs is carried out based on closed-loop control systems, as shown in Fig. 2. For this, first the system state-space description is given as (5) and (12). Then, for voltage control, an LQR-based control technique is utilized to provide an acceptable level of voltage tracking at the output of the DSTATCOM filter. For current control, a pole-shift technique is utilized to provide an acceptable level of current tracking at the output of DSTATCOM filter. The controller parameters are calculated by solving (9) and (15). In each case, the error between the reference and the actual values are passed through a hysteresis controller to generate the proper Turn On/Off gate signals for the IGBTs of the VSCs, as given in (10). This is a per-phase control and a similar control technique is utilized for each phase of the DSTATCOM individually.

5. Case studies and simulation results

Several case studies are carried out in PSCAD/EMTDC when a DSTATCOM is connected both in LV and MV feeders, with the control techniques discussed in the previous two sections. The DSTATCOM connection for LV and MV systems are shown respectively in Fig. 3(a) and (b). The technical data are given in Tables 1 and 2 in Appendix A.1. These case studies are discussed below. It is to be noted that in these case studies, the loads are modelled only as constant impedance loads. Although the electrical loads can be assumed as constant impedance, constant power or constant current types, this will have negligible effect on the control and performance of the proposed DSTATCOM.

5.1. LV application of DSTATCOM

5.1.1. Case-1

Let us consider the LV feeder of Fig. 3 (a), with a Δ/Y transformer and unbalanced loads where a DSTATCOM, with the topology shown in Fig. 1(a), is installed and controlled based on the voltage control strategy described in Section 3.1. The steady-state, three-phase instantaneous current waveform in the upstream feeder, downstream load and the output of the DSTATCOM are shown in Fig. 4(a–c), respectively. The phase active power flow along the above-mentioned locations is shown in Fig. 4(d–f). Separate

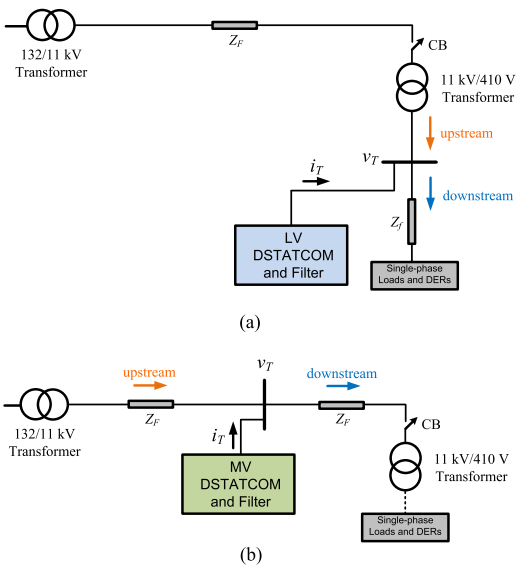

Fig. 3. Schematic diagram of a distribution network with DSTATCOM installed in: (a) LV feeder and (b) MV feeder.

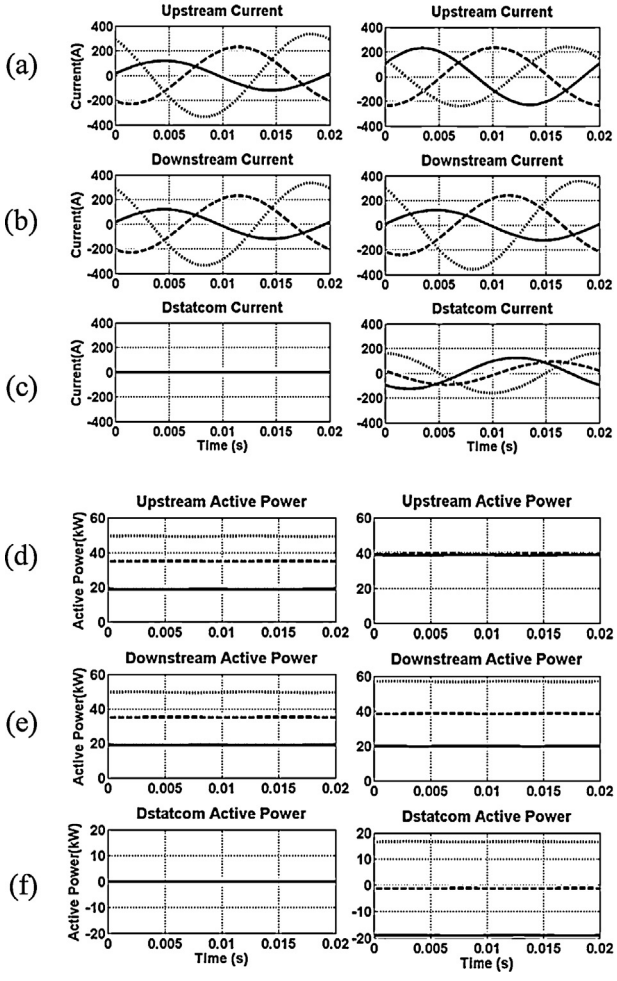

Fig. 4. Case-1 simulation results before DSTATCOM connection (left column) and after DSTATCOM connection (right column). (solid line: Phase-A, dashed line: Phase-B, dotted line: Phase-C).

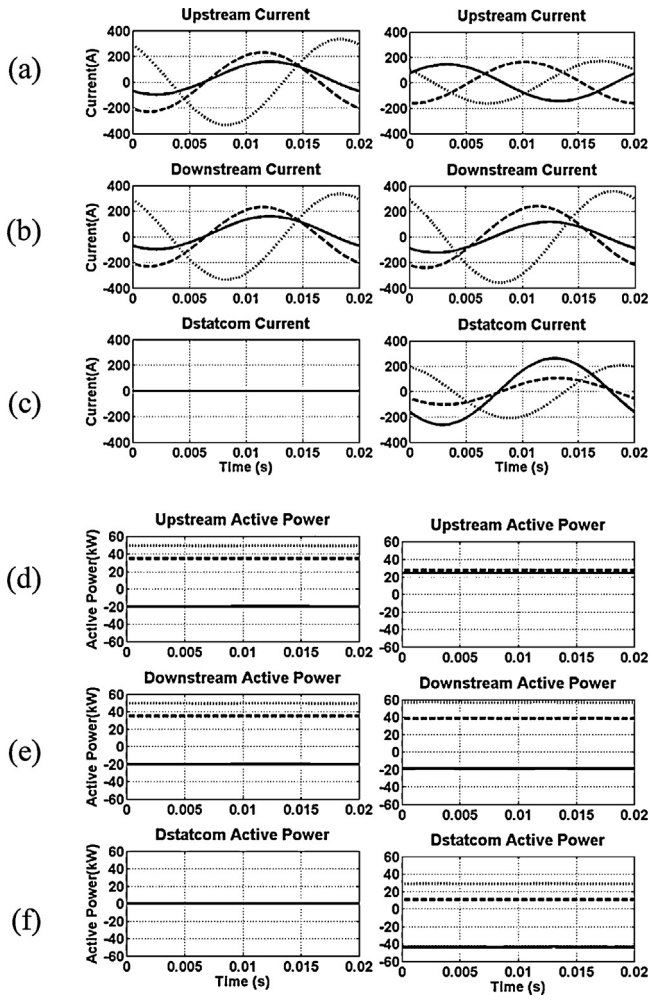

Fig. 5. Case-2 simulation results before DSTATCOM connection (left column) and after DSTATCOM connection (right column). (solid line: Phase-A, dashed line: Phase-B, dotted line: Phase-C).

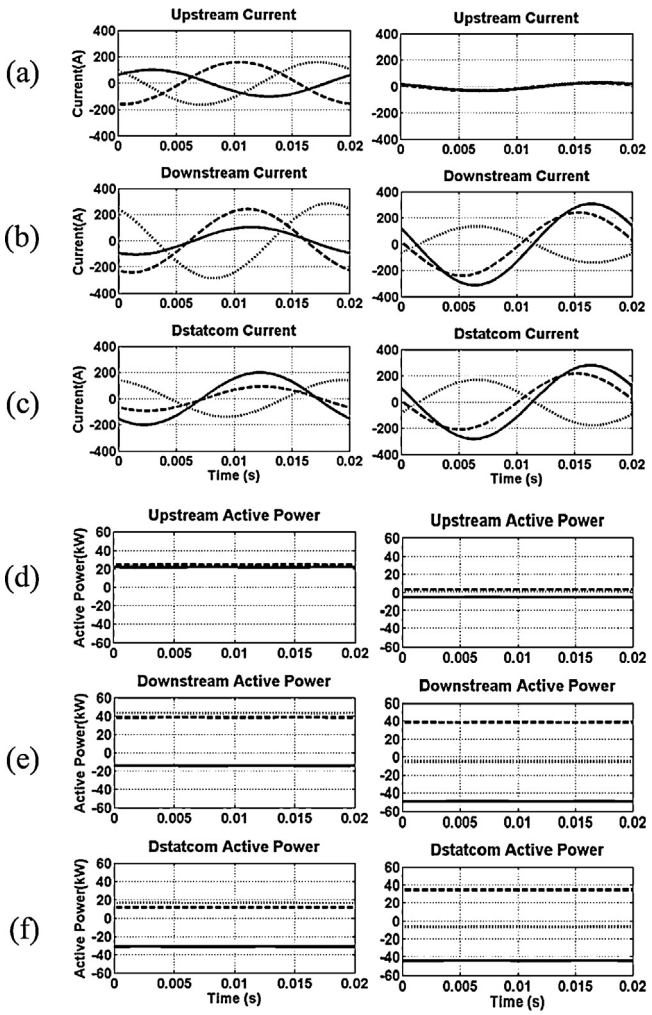

Fig. 6. Case-3 simulation results in grid-connected mode (left column) and off-grid mode (right column) operation of the LV feeder while the DSTATCOM is connected to the LV feeder in both modes (solid line: Phase-A, dashed line: Phase-B, dotted line: Phase-C).

results are shown for the cases before and after connection of the DSTATCOM. The upstream currents are unbalanced due to the unbalanced downstream currents (Fig. 4a, b-left). The active power flow in the upstream of DSTATCOM is equal to the downstream (Fig. 4d, e-left). After the DSTATCOM is connected to the feeder, the unbalanced currents are only observed at the downstream side (Fig. 4b-right) while the upstream currents get balanced (Fig. 4a-right). Similarly, the active power flow in the DSTATCOM upstream is balanced (Fig. 4d-right) while the downstream side is still unbalanced (Fig. 4e-right). It is to be noted that since the loads in these simulation results are assumed to be constant impedance loads, the downstream power before and after DSTATCOM connection is slightly modified due to the voltage correction by the DSTATCOM. In this scenario, since no reverse power flow is observed in any of the phases, the DSTATCOM only facilitates a set of balanced currents in its upstream. The output currents and active power flow from the DSTATCOM are shown in Fig. 4c, f-right.

5.1.2. Case-2

Now, let us consider the network discussed in case-1 with a reverse power flow in phase-A due to the connection of excessive single-phase generation to this phase. The simulation results are shown in Fig. 5. The active power flow in the feeder is −20, 35 and 49 kW respectively in phase-A, B and C (Fig. 5d-left). After the DSTATCOM connection, the active power flow in the DSTATCPOM upstream is 27 kW in all phases (Fig. 5d-right). This is achieved as the DSTATCOM absorbs 43 kW from phase-A and injects 10 and 28.5 kW respectively to phase-B and C (Fig. 5f-right). Due to the proper power circulation through the DSTATCOM, a set of balanced phase current is also observed in the upstream feeder after the DSTATCOM (Fig. 5a-right). This case study demonstrates the principle of power circulation through the DSTATCOM which is based on absorbing active power from the phase with reverse flowing power and injecting that power (minus DSTATCOM internal losses) to the other phases. The summation of the active powers at the outputs of the DSTATCOM represents the internal losses of the DSTATCOM (Fig. 5f-right). In this case, the DSTATCOM loss is equal to 4.5 kW.

5.1.3. Case-3

Now, let us consider the same network as in case-2, when it is operated in an islanded (off-grid) mode, i.e. the circuit breaker CB is assumed to be open. In this case, the single-phase DERs are droop controlled as discussed in Appendix A.2. In [51], it is shown that under such a condition, the distribution transformer provides a power circulation path. Hence, a single-phase DER connected to one phase supplies a load in another phase through the transformer. Since this has been discussed in detail in [51], it is not repeated here as it is not the main focus of this paper. The simulation results are shown in Fig. 6 separately for grid-connected and off-grid modes, where in both modes the DSTATCOM is connected to the LV feeder.

In grid-connected mode, due to the presence of the DSTATCOM, a set of balanced currents are observed in the upstream of the DSTATCOM (Fig. 6a-left). Although an active power flow of −14, 38 and −43 kW is respectively observed in phase-A, B and C in the DSATCOM downstream (Fig. 6e-left), due to the presence of the DSTATCOM, an active power of approximately 20 kW is observed in all phases in the DSTATCOM upstream (Fig. 6d-left). It can be seen that in this case, the DSTATCOM absorbs 31.6 kW from phase-A and injects 11.4 and 16.0 kW respectively to phase-B and C (Fig. 6f-left). After the grid is isolated, the upstream currents are only the magnetizing currents of the transformer and are negligible (Fig. 6a-right). Due to the Δ/Y configuration of the transformer, a very small circulating current and power is observed in the DSTATCOM upstream (Fig. 6d-right). In such a case, the voltage-droop controlled DERs in phase-A, increase their generation and hence a −50.5 kW power flow is observed in this phase in the downstream of DSTATCOM (Fig. 6e-right). This power is circulated through the DSTATCOM to the other phases. Hence, the DSTATCOM absorbs 45 and 7.7 kW from phase-A and C and injects 34 kW to phase-B (Fig. 6f-right).

This case study demonstrates that the proposed DSTATCOM can help the LV network with sufficient DERs to operate in off-grid mode. In such a case, the DSTATCOM provides a path for the extra generated power by the DERs to flow into the phases with power deficiency.

5.2. MV application of DSTATCOM

5.2.1. Case-4

Now, let us consider a MV feeder of Fig. 3(b) with unbalanced loads where a DSTATCOM, with the topology shown in Fig. 1(a), is installed and controlled based on voltage control strategy. The simulation results are shown in Fig. 7. Before the DSTATCOM connection, the upstream currents are unbalanced and equal to those at the downstream of the DSTATCOM (Fig. 7a, b-left). Similarly, the active power flow in each phase is different (Fig. 7d-left). However, no reverse power flow is observed in any of the phases. Hence, the DSTATCOM only has to facilitate a set of balanced currents in its upstream. After the DSTATCOM is connected to the feeder, its upstream currents are balanced (Fig. 7a-right) while its downstream remains unbalanced (Fig. 7b-right). Similarly, the active power flow in the DSTATCOM upstream becomes equal to 4 MW in all phases (Fig. 7d-right) while those in the downstream side remain unbalanced (Fig. 7e-right). The output currents and active power flow from the DSTATCOM are shown in Fig. 7c, f-right.

5.2.2. Case-5

Now, let us consider utilizing a DSTATCOM, with the topology shown in Fig. 1(b), in the MV network of case-4, operating in voltage control strategy. In this configuration, the filter capacitor has an LV rating. Before DSTATCOM connection, the currents in DSTATCOM upstream are unbalanced (Fig. 8a-left). After the DSTATCOM connection, the actual and reference values of voltage across the filter capacitor are shown together in Fig. 8b-left and the tracking error is shown Fig. 8b-right. From this figure, it can be seen that the tracking error of the controller is about 8 V peak to peak. However, the upstream current is not balanced (Fig. 8a-right), as discussed earlier in Section 3(B). Hence, for this configuration of DSTATCOM, voltage control strategy fails.

5.2.3. Case-6

Now, let us consider the network and DSTATCOM of case-5, where a current control strategy, as discussed in Section 3.2 is utilized instead of the voltage control strategy. The simulation results are shown in Fig. 9.

As it can be seen from the results, before the DSTATCOM connection, the currents at the upstream and downstream of the

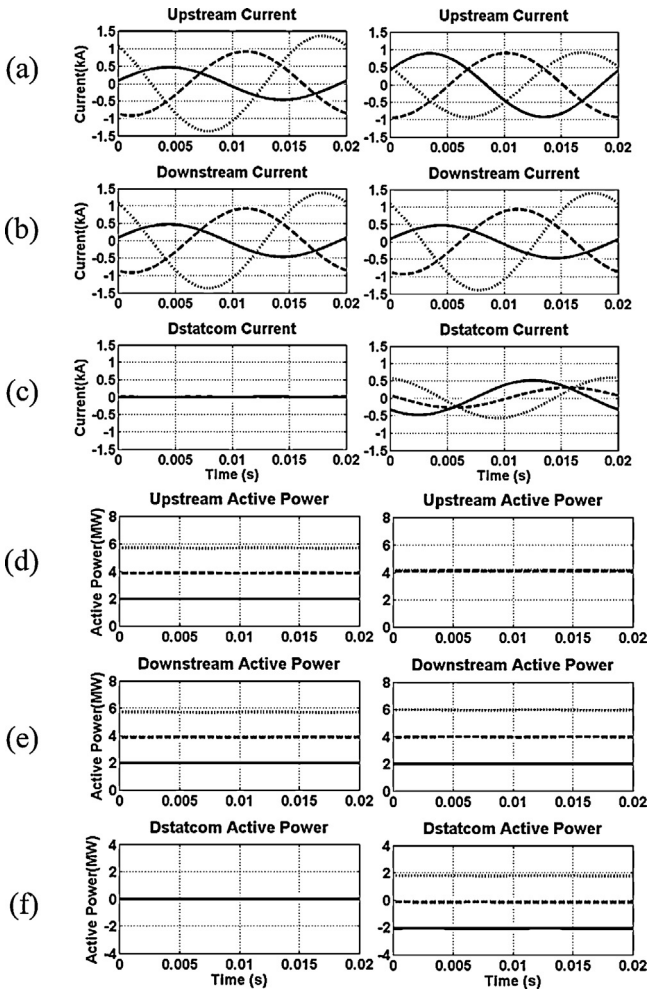

Fig. 7. Case-4 simulation results before DSTATCOM connection (left column) and after DSTATCOM connection (right column). (solid line: Phase-A, dashed line: Phase-B, dotted line: Phase-C).

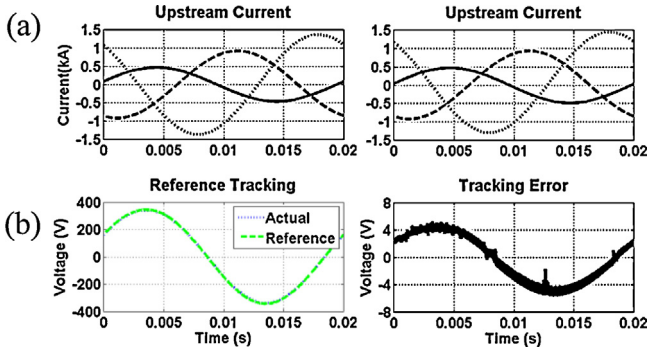

Fig. 8. Case-5 simulation results: Top row: Upstream current before DSTATCOM connection (left) and after its connection (right), Bottom row: DSTATCOM output voltage and its reference (left) and DSTATCOM output voltage tracking error (right) (solid line: Phase-A, dashed line: Phase-B, dotted line: Phase-C).

DSTATCOM are unbalanced (Fig. 9a, b-left). The active power flow is 2.8, 2.3 and 1.5 MW respectively in phase-A, B and C (Fig. 9d-left). After the DSTATCOM connection, the upstream current becomes balanced (Fig. 9a-left) and the active power becomes 2.3 MW in all phases (Fig. 9d-right). This is achieved as the DSTATCOM absorbs 1.18 MW from phase-C and injects 1.16 MW to phase-A while it has no power exchange with phase-B (Fig. 9f-right). In this case, the DSTATCOM has a loss of 20 kW, since it is connected to an MV feeder.

Table 1
Summary of the simulation results.

Simulation case no.	DSTATCOM connection	DSTATCOM filter type	Control strategy	Summary	Result
1	LV	LC (LV rating)	Voltage	The LV network contains unbalanced loads	Proper power circulation through the DSTATCOM Balanced currents in the DSTATCOM upstream
2	LV	LC (LV rating)	Voltage	The LV network contains unbalanced loads and unbalanced single-phase DERS	Proper power circulation through the DSTATCOM Balanced currents in the DSTATCOM upstream
3	LV	LC (LV rating)	Voltage	The grid in this case is isolated. DERs are only available in phase-A and C while unbalanced loads are distributed in all phases	Proper power circulation through the DSTATCOM DERs in phase-A and C supply the load in phase-B through DSTATCOM
4	MV	LC (MV rating)	Voltage	The MV network experiences unbalanced loads and unbalanced generations	Proper power circulation through the DSTATCOM Balanced currents in the DSTATCOM upstream
5	MV	LCL (LV rating)	Voltage	Same Network as Case-4	Unbalanced currents in the DSTATCOM upstream
6	MV	LCL (LV rating)	Current	Same network as case-4	Proper power circulation through the DSTATCOM Balanced currents in the DSTATCOM upstream

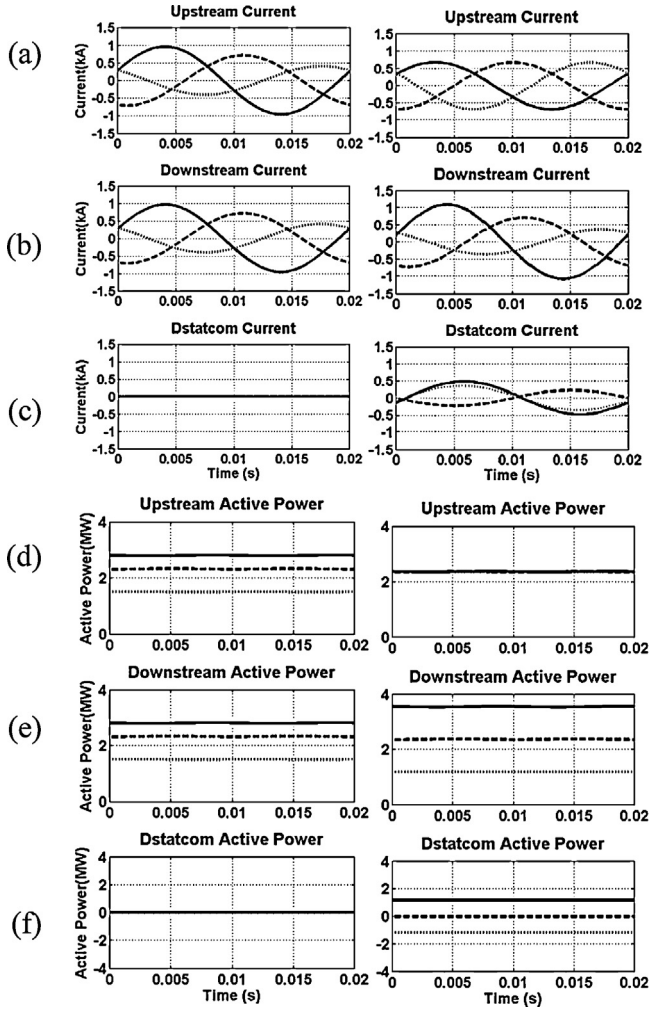

Fig. 9. Case-6 simulation results before DSTATCOM connection (left column) and after DSTATCOM connection (right column). (solid line: Phase-A, dashed line: Phase-B, dotted line: Phase-C).

5.3. Simulation results and discussion

Based on the above simulation cases, it can be seen that for a DSTATCOM connected in LV feeder, a filter type of LC with a voltage control strategy can properly circulate the reverse power flow and balance the upstream currents (as illustrated in Case-2). In the situations in which no reverse power flow is observed in any of the phases, the DSTATCOM will only facilitate a set of balanced currents in its upstream (as illustrated in Case-1). The DSTATCOM with a voltage control technique connected to the LV feeder, as proposed in this paper, can facilitate off-grid operation mode for the system, providing that the DERs have adequate capability to supply the local loads within the LV feeder (as illustrated in Case-3).

Similarly, it is realized that for a DSTATCOM connected in MV feeder, a filter type of LC with a voltage control strategy can only be successful if the filter has MV rating (as illustrated in Case-4). To utilize a filter with LV rating, the LCL filter with a voltage control strategy was shown to be unsuccessful in making the upstream currents balanced (as illustrated in Case-5). However, when a current control strategy is used instead of the voltage control strategy, the DSTATCOM is successful for proper circulation of the reverse power flow and balancing the upstream currents (as illustrated in Case-6). This is summarized in Table 1.

6. Conclusions

Large number of single- phase DERs, installed in one phase, can result in reverse power flow in that phase if the generation capacity is higher than the phase load demand. In this paper, two different topologies are discussed for power circulation through a DSTATCOM in order to prevent the reverse power flowing into the upstream network. The proposed DSTATCOM is composed of a VSC with an LC filter, either connected directly to the LV feeder or through a boosting transformer in case of the MV feeder. The simulation results show that a voltage control strategy is effective for circulating the phase surplus power through the DSTATCOM in the LV network while it fails for MV applications due to the leakage inductance of the boosting transformers. Hence a current control strategy is a preferred option for this case.

Appendix.

A.1. Technical parameters of the network

The data of the network in Figs. 1 and 3 are listed in Tables 2 and 3.

Table 2
Technical data of the network in simulation cases 1–3.

MV feeder	11 kV L–L, 50 Hz, $R = 0.5\ \Omega$, $X = 1.57\ \Omega$
Distribution transformer	100 kVA, 11 kV/410 V, 50 Hz, $Z_t = 10\%$
LV feeder	410 V L–L, 50 Hz, $R = 0.022\ \Omega$, $X = 0.022\ \Omega$
Three-phase LV load	$S_A = 19.5 + j\,6.3$, $S_B = 38.6 + j\,13$, $S_C = 53 + j\,19.2$ kVA
DER for Case-2	One single-phase DER with $P = 40$ kW, PF = 1, connected to phase-A
DERs for Case-3	2 single phase DERs with $P_{rated} = 50$ kW, $S_{rated} = 60$ kVA with $L_{coupling} = 450\ \mu$H (connected to phase-A) and $L_{coupling} = 680\ \mu$H (connected to phase-C)
DSTATCOM	$R_f = 0.1\ \Omega$, $L_f = 4$ mH, $C_f = 25\ \mu$F, $V_{dc} = 1$ kV, $a = 1$, $h = 10^{-4}$ $K = [1.5463\ -0.7092]$

Table 3
Technical data of the network in simulation cases 4–6.

HV feeder	132 kV L–L, 50 Hz, $R = 0.25\ \Omega$, $X = 3.14\ \Omega$
Transformer	15 MVA, 132/11 kV, 50 Hz, $Z_t = 5\%$
MV feeder	11 kV L–L, 50 Hz, $R = 0.5\ \Omega$, $X = 1.57\ \Omega$
Three-phase MV load	$S_A = 2 + j\,0.66$, $S_B = 4 + j\,1.33$, $S_C = 6 + j\,2$ MVA
DER for Case-6	One single-phase DER with $P = 0.45$ MW, PF = 1, connected to phase-A
DSTATCOM for Case-4	$R_f = 0.1\ \Omega$, $L_f = 4$ mH, $C_f = 25\ \mu$F, $V_{dc} = 13$ kV, $a = 1$, $h = 10^{-4}$ $K = [1.5463\ -0.7092]$
DSTATCOM for Cases-5 and 6	$R_f = 0.1\ \Omega$, $L_f = 4$ mH, $C_f = 25\ \mu$F, $V_{dc} = 1$ kV, $a = 11$, $h = 10^{-4}$ $\frac{S(z^{-1})}{R(z^{-1})} = \frac{43.8019 - 85.4746z^{-1} + 41.7269z^{-2}}{1 - 0.1237z^{-1} - 0.025z^{-2}}$

A.2. Control of LV networks operating in islanded mode

A LV feeder is considered with two DERs. Let us assume that each DER is supplied by a DC source and is connected through an H-bridge VSC, an LC filter and an impedance of $j\omega L_{coup}$ to the LV feeder. The active power (p) and reactive power (q) supplied by the DER to the LV feeder are then given by [47]

$$p = \frac{|V_T| \times |V_{cf}|}{\omega L_T} \sin(\delta_{cf} - \delta_T)$$
$$q = \frac{|V_T|}{\omega L_T} \left(|V_{cf}| \cos(\delta_{cf} - \delta_T) - |V_T| \right) \tag{A.1}$$

where V_T and V_{cf} are respectively the LV feeder side and LC filter voltage of the coupling impedance and $V = |V|\ \angle\delta$ is the phasor representation of $v(t)$.

In islanded mode, it is assumed that the frequency of the LV feeder reduces by $\Delta\omega$, as the DER increases its output active power from zero to its rated value. Hence, P–δ droop coefficient for the DER is

$$m = \frac{\Delta\omega}{P_{rated}} \tag{A.2}$$

Assuming $\Delta\omega$ to be constant for both of the DERs with different ratings, the ratio of P–δ droop coefficient between the two DERs is

$$\frac{m_1}{m_2} = \frac{P_{rated,2}}{P_{rated,1}} \tag{A.3}$$

Similarly, it is assumed that the voltage of the LV feeder reduces by ΔV, when the DER increases its output reactive power from zero to its rated value. Hence, the Q-V droop coefficient for the DER is

$$n = \frac{\Delta V}{Q_{rated}} \tag{A.4}$$

Assuming ΔV to be constant for both of the DERs with different ratings, the ratio of Q–V droop coefficient between two DERs is

$$\frac{n_1}{n_2} = \frac{Q_{rated,2}}{Q_{rated,1}} \tag{A.5}$$

In [47], it was shown that the output active ratio and reactive power ratio among two DERs are the same as the ratio of their rated active and reactive powers as

$$\frac{P_1}{P_2} \approx \frac{m_2}{m_1}, \quad \frac{Q_1}{Q_2} \approx \frac{n_2}{n_1} \tag{A.6}$$

On the other hand, in parallel operation of converter-interfaced DERs in an islanded network, it is desired that the voltage angle difference on two sides of the coupling inductance (i.e. $\delta_{cf} - \delta_T$) in (A.1) to be a small value so that it is on the linear section of sinusoidal P–δ characteristic of (A.1). Similarly, it is desired that the voltage drop across the coupling inductance (i.e. $|V_{cf}| - |V_T|$) in (A.1) to be small (i.e. 1–2%). For achieving these assumptions, the coupling inductances are designed inversely proportional to the rated power of DERs as [47]

$$\frac{L_{coup,1}}{L_{coup,2}} = \frac{P_{rated,2}}{P_{rated,1}} = \frac{Q_{rated,2}}{Q_{rated,1}} \tag{A.7}$$

References

[1] L. Byrnes, C. Brown, J. Foster, L.D. Wagner, Australian renewable energy policy: barriers and challenges, Renew. Energy 60 (December) (2013) 711–721.
[2] M.A. Abdullah, A.P. Agalgaonkar, K.M. Muttaqi, Climate change mitigation with integration of renewable energy resources in the electricity grid of New South Wales, Australia, Renew. Energy 66 (June) (2014) 305–313.
[3] A. Aslani, K.F.V. Wong, Analysis of renewable energy development to power generation in the United States, Renew. Energy 63 (March) (2014) 153–161.
[4] S. Spiecker, C. Weber, The future of the European electricity system and the impact of fluctuating renewable energy – a scenario analysis, Energy Policy 65 (February) (2014) 185–197.
[5] R. Sen, S.C. Bhattacharyya, Off-grid electricity generation with renewable energy technologies in India: an application of HOMER, Renew. Energy 62 (February) (2014) 388–398.
[6] Z. Ming, L. Ximei, L. Yulong, P. Lilin, Review of renewable energy investment and financing in China: status, mode, issues and countermeasures, Renew. Sustain. Energy Rev. 31 (March) (2014) 23–37.
[7] A. Zahedi, Development of an economical model to determine an appropriate feed – in tariff for grid-connected solar PV electricity in all states of Australia, Renew. Sustain. Energy Rev. 13 (May (4)) (2009) 871–878.
[8] A. Bahadori, C. Nwaoha, A review on solar energy utilisation in Australia, Renew. Sustain. Energy Rev. 18 (February) (2013) 1–5.
[9] R.J. Davy, A. Troccoli, Interannual variability of solar energy generation in Australia, Solar Energy 86 (December (12)) (2012) 3554–3560.
[10] C.W. Hsu, Using a system dynamics model to assess the effects of capital subsidies and feed-in tariffs on solar PV installations, Appl. Energy 100 (December) (2012) 205–217.
[11] J.L. Silveira, C.E. Tuna, W. de Queiroz Lamas, The need of subsidy for the implementation of photovoltaic solar energy as supporting of decentralized electrical power generation in Brazil, Renew. Sustain. Energy Rev. 20 (April) (2013) 133–141.
[12] A. Macintosh, D. Wilkinson, Searching for public benefits in solar subsidies: a case study on the Australian government's residential photovoltaic rebate program, Energy Policy 39 (June (6)) (2011) 3199–3209.
[13] S. Srinivasan, Subsidy policy and the enlargement of choice, Renew. Sustain. Energy Rev. 13 (December (9)) (2009) 2728–2733.
[14] S.B. Peterson, J.J. Michalek, Cost-effectiveness of plug-in hybrid electric vehicle battery capacity and charging infrastructure investment for reducing US gasoline consumption, Energy Policy January (52) (2013) 429–438.
[15] R.M. Krause, S.R. Carley, B.W. Lane, J.D. Graham, Perception and reality: public knowledge of plug-in electric vehicles in 21 U.S. cities, Energy Policy 63 (December) (2013) 433–440.
[16] F. Shahnia, A. Ghosh, G. Ledwich, F. Zare, Predicting voltage unbalance impacts of plug-in electric vehicles penetration in residential low voltage distribution networks, Electr. Power Compon. Syst. 41 (October (16)) (2013) 1594–1616.
[17] B.K. Sovacool, R.F. Hirsh, Beyond batteries: an examination of the benefits and barriers to plug-in hybrid electric vehicles (PHEVs) and a vehicle-to-grid (V2G) transition, Energy Policy 37 (March (3)) (2009) 1095–1103.
[18] J.D.K. Bishop, C.J. Axon, D. Bonilla, et al., Evaluating the impact of V2G services on the degradation of batteries in PHEV and EV, Appl. Energy 111 (November) (2013) 206–218.
[19] K.C. Divya, J. Østergaard, Battery energy storage technology for power systems – an overview, Electr. Power Syst. Res. 79 (April (4)) (2009) 511–520.

[20] A. Purvins, I.T. Papaioannou, L. Debarberis, Application of battery-based storage systems in household demand smoothening in electricity distribution grids, Energy Convers. Manag. 65 (January) (2013) 272–284.
[21] N.K.C. Nair, N. Garimella, Battery energy storage systems: assessment for small-scale renewable energy integration, Energy Build. 42 (November (11)) (2010) 2124–2130.
[22] D. Parra, G.S. Walker, M. Gillott, Modeling of PV generation, battery and hydrogen storage to investigate the benefits of energy storage for single dwelling, Sustain. Cities Soc. 10 (February) (2014) 1–10.
[23] J.A. Peças Lopes, N. Hatziargyriou, J. Mutale, et al., Integrating distributed generation into electric power systems: a review of drivers, challenges and opportunities, Electr. Power Syst. Res. 77 (July (9)) (2007) 1189–1203.
[24] W. El-Khattam, M.M.A. Salama, Distributed generation technologies, definitions and benefits, Electr. Power Syst. Res. 71 (October (2)) (2004) 119–128.
[25] J.C. Hernández, F.J.R. Rodriguez, F. Jurado, Technical impact of photovoltaic distributed generation on radial distribution systems: stochastic simulations for a feeder in Spain, Int. J. Electr. Power Energy Syst. 50 (September) (2013) 25–32.
[26] R.A. Walling, R. Saint, R.C. Dugan, J. Burke, L.A. Kojovic, Summary of distributed resources impact on power delivery systems, IEEE Trans. Power Deliv. 23 (2008) 1636–1644.
[27] F. Shahnia, R. Majumder, A. Ghosh, G. Ledwich, F. Zare, Voltage imbalance analysis in residential low voltage distribution networks with rooftop PVs, Electr. Power Syst. Res. 81 (2011) 1805–1814.
[28] F. Shahnia, A. Ghosh, Decentralized voltage support in a low voltage feeder by droop based voltage controls PVs, in: Proc. of 23rd Australasian Universities Power Engineering Conference (AUPEC), September. Hobart, Australia, 2013.
[29] M. Hamzeh, H. Karimi, H. Mokhtari, A new control strategy for a multi-bus MV microgrid under unbalanced conditions, IEEE Trans. Power Syst. 27 (November (4)) (2012) 2225–2232.
[30] A. Ghosh, G. Ledwich, Power Quality Enhancement using Custom Power Devices, Kluwer Academic, Boston, 2002.
[31] F. Shahnia, A. Ghosh, G. Ledwich, F. Zare, Voltage unbalance improvement in low voltage residential feeders with rooftop PVs using custom power devices, Int. J. Electr. Power Energy Syst. 55 (February) (2014) 362–377.
[32] B. Han, B. Bae, S. Baek, G. Jang, New configuration of UPQC for medium-voltage application, IEEE Trans. Power Deliv. 21 (July (3)) (2006) 1438–1444.
[33] Y. Li, D.M. Vilathgamuwa, P.C. Loh, Microgrid power quality enhancement using a three-phase four-wire grid-interfacing compensator, IEEE Trans. Ind. Appl. 41 (November/December (6)) (2005) 1707–1719.
[34] J. Guerrero, M. Chandorkar, T. Lee, P. Loh, Advanced control architectures for intelligent microgrids. Part II: Power quality, energy storage, and AC/DC microgrids, IEEE Trans. Ind. Electron. 60 (April (4)) (2013) 1263–1270.
[35] M. Brenna, R. Faranda, E. Tironi, A new proposal for power quality and custom power improvement: open UPQC, IEEE Trans. Power Deliv. 24 (October (4)) (2009) 2107–2116.
[36] H.M. Wijekoon, D.M. Vilathgamuwa, S.S. Choi, Interline dynamic voltage restorer: an economical way to improve interline power quality, IEE Proc. Gener. Trans. Distrib. 150 (September (5)) (2003) 513–520.
[37] A.K. Jindal, A. Ghosh, A. Joshi, Interline unified power quality conditioner, IEEE Trans. Power Deliv. 22 (1) (2007) 364–372.
[38] T. Zaveri, B. Bhalja, N. Zaveri, Comparison of control strategies for DSTATCOM in three-phase, four-wire distribution system for power quality improvement under various source voltage and load conditions, Int. J. Electr. Power Energy Syst. 43 (December (1)) (2012) 582–594.
[39] B. Singh, P. Jayaprakash, D.P. Kothari, New control approach for capacitor supported DSTATCOM in three-phase four wire distribution system under non-ideal supply voltage conditions based on synchronous reference frame theory, Int. J. Electr. Power Energy Syst. 33 (Jume (5)) (2011) 1109–1117.
[40] D. Sreenivasarao, P. Agarwal, B. Das, A T-connected transformer based hybrid DSTATCOM for three-phase, four-wire systems, Int. J. Electr. Power Energy Syst. 44 (January (1)) (2013) 964–970.
[41] S. Mazumder, A. Ghosh, F. Shahnia, F. Zare, G. Ledwich, Excess power circulation in distribution networks containing distributed energy resources, in: IEEE Power and Energy Society General Meeting (PES), July. San Diego, USA, 2012, pp. 1–8.
[42] F. Shahnia, A. Ghosh, G. Ledwich, F. Zare, An approach for current balancing in distribution networks with rooftop PVs, in: IEEE Power and Energy Society General Meeting (PES), July. San Diego, USA, 2012, pp. 1–6.
[43] Olex Aerial Catalogue, http://www.olex.com.au/Australasia/2012/OLC12641_AerialCat.pdf
[44] A. Ghosh, A. Joshi, A new approach to load balancing and power factor correction in power distribution system, IEEE Trans. Power Deliv. 15 (2000) 417–422.
[45] A. Ghosh, A.K. Jindal, A. Joshi, Inverter control using output feedback for power compensating devices, IEEE Asia-Pacific Region-10 Conf. (TENCON) 1 (2003) 48–52.
[46] A. Ghosh, G. Ledwich, Load compensating DSTATCOM in weak AC systems, IEEE Trans. Power Deliv. 18 (2003) 1302–1309.
[47] F. Shahnia, R.P.S. Chandrasena, S. Rajakaruna, A. Ghosh, Primary control level of parallel distributed energy resources converters in system of multiple interconnected autonomous microgrids within self-healing networks, IET Gener. Trans. Distrib. 8 (February (2)) (2014) 203–222.
[48] M. Gopal, Digital Control and State Variable Methods, Tata McGraw-Hill, India, 2009.
[49] A. Tewari, Modern Control Design with Matlab and Simulink, Wiley, India, 2002.
[50] G. Ramakrishna, O.P. Malik, Radial basis function identifier and pole-shifting controller for power system stabilizer application, IEEE Trans. Energy Convers. 19 (December (4)) (2004) 663–670.
[51] R.P.S. Chandrasena, F. Shahnia, S. Rajakaruna, A. Ghosh, Operation and control of three phase microgrids consisting of single-phase DERs, in: Proc. of 8th IEEE International Conference on Industrial and Information Systems, December. Kandy, Sri Lanka, 2013.